

Article

Digital Twin of a Hydraulic System with Leak Diagnosis Applications

Leonardo Gómez-Coronel ¹, Ildeberto Santos-Ruiz ¹, Lizeth Torres ², Francisco-Ronay López-Estrada ^{1,*}, Samuel Gómez-Peñate ¹ and Elías Escobar-Gómez ¹

¹ TURIX-Dynamics Diagnosis and Control Group, Tecnológico Nacional de México, IT Tuxtla Gutiérrez Chiapas, Tuxtla Gutiérrez 29050, Mexico; m16270670@tuxtla.tecnm.mx (L.G.-C.); ildeberto.dr@tuxtla.tecnm.mx (I.S.-R.); samuel.gp@tuxtla.tecnm.mx (S.G.-P.); enescobarg@tuxtla.tecnm.mx (E.-E.G.)

² Instituto de Ingeniería, Universidad Nacional Autónoma de México, Ciudad de México 04510, Mexico; forreso@iingen.unam.mx

* Correspondence: frlopez@ittg.edu.mx

Abstract: This paper presents the design and development of a digital twin to diagnose leaks in water distribution networks. The digital twin allows for the remote operation of the hydraulic system's actuators using embedded microcontrollers integrated with Internet of Things (IoT) capabilities. Pressure head and flow rate measurements are received online in the operator interface, and hydraulic simulations are performed with a well-calibrated EPANET model of the hydraulic system to estimate the pressure head at nodes without sensors. A genetic algorithm was designed to detect and estimate the size of the leaks online. Different experiments were carried out to validate the online application of the method based on the digital twin and under a multi-leak event.

Keywords: digital twin; leak diagnosis; fault diagnosis; Internet of Things; hydraulic system



Citation: Gómez-Coronel, L.; Santos-Ruiz, I.; Torres, L.; López-Estrada, F.R.; Gómez-Peñate, S.; Escobar-Gómez, E. Digital Twin of a Hydraulic System with Leak Diagnosis Applications. *Processes* **2023**, *11*, 3009. <https://doi.org/10.3390/pr11103009>

Academic Editors: Stefania Tronci, Massimiliano Errico, Riccardo Bacci Di Capaci, Ingmar Nopens, Elena Torfs and Michael Short

Received: 26 September 2023

Revised: 13 October 2023

Accepted: 17 October 2023

Published: 19 October 2023



Copyright: © 2023 by the authors. Licensee MDPI, Basel, Switzerland. This article is an open access article distributed under the terms and conditions of the Creative Commons Attribution (CC BY) license (<https://creativecommons.org/licenses/by/4.0/>).

1. Introduction

Water distribution networks are exposed to many factors that produce leaks, such as corrosion, wear, poor installation, or adverse environmental conditions. Corrective and predictive maintenance can reduce the occurrence of leak events. A study by the Organization for Economic Co-operation and Development (OECD) [1,2] showed that the global volumetric percentage of water lost due to leaks is close to 21%. Among the different countries in the study, Mexico experiences a more critical situation since this percentage ascends to approximately 40%. This is why leaks must be promptly detected and repaired to minimize their negative associated economic cost and environmental pollution. This problem increases because most water distribution systems have their pipes underground, making it more complex and sometimes impossible to identify the leak, which increases their lifetime [3]. However, in some nodes, knowledge of the hydraulic variables during the system's operation, such as pressure head and flow rate, can be used to identify abnormal operating conditions associated with the leak. Furthermore, implementing intelligent systems that perform constant real-time monitoring and prognosis of the operating conditions of the hydraulic system can complement online leak detection, isolation, and diagnosis.

In recent years, intelligent systems have been developed that integrate physical and virtual environments into cyber-physical systems. This trend has been significantly propelled by technological advancements like the Internet of Things (IoT) and the continuous enhancement of intelligent sensors and actuators. These systems are known as an intelligent water distribution network (IWDN) [4], and their purpose is to monitor hydraulic demand and interact with valves to respond to specific water demand requirements efficiently. An IWDN has also been used to monitor quality parameters by including sensors, a communication network, and computing technologies to construct software models that

manage data transfer and execute data analysis algorithms [5]. The work performed by [6] explored an evolution of the traditional methods in water quality monitoring by including an alarm-emitting capacity if the measured parameters were not under specific ranges. Similarly, the author in [7] applied the IoT to monitor and control hydraulic and quality variables in a district-metered area of Guanajuato in Mexico. From a safety point of view, in [8] an IoT-based system was designed to manage a water distribution network with the capability to respond and alert the user concerning abnormal operating conditions such as leaks and even cyber-attacks. Similarly, in [9,10], it was demonstrated how an IoT-based system integrated with cloud computing could solve problems related to risk management of a potable water treatment plant. The authors in [11] developed an IoT system for intelligent water management to provide a constant water supply in places where tanks, motors, and pumps are scarce.

Recently, the authors of [12] introduced a novel approach involving the use of a new class of IWDN known as a digital twin, which can be seen as a virtual replica of a physical WDN, used for real-time monitoring, simulation, and analysis to enhance performance and decision-making. As part of their research, the authors successfully developed and implemented a digital twin model for the district-metered area of Valencia, Spain, whose main characteristics are fidelity in the representation of the physical system, low latency, remote control, precise simulation of any desired operating condition, reliable sensors, and real-time monitoring of the operating conditions and water consumption. By following this approach, in [13], a digital twin was designed for the water distribution system of Lisbon in Portugal. These macro implementations demonstrated the practice of *digital twins*, which provided valuable information concerning the users' consumption habits, which change according to the hour of the day and the year's season. In [14], a digital twin of the city of Lakewood, California, was used to analyze its feasibility in risk management during emergencies by studying changes in the consumption patterns during the COVID-19 pandemic period. All previous investigations demonstrate how real-life implementations of *digital twins* on water distribution networks are a growing interest in academia and industry. Nonetheless, to the authors' knowledge, no reported practical implementations of *digital twins* are dedicated to implementing online remote leak diagnosis.

The main contribution presented in this paper is the implementation of a digital twin of an experimental hydraulic system dedicated to diagnosing single- and multi-leak events using a genetic algorithm (GA) and IoT technologies. The proposed system integrates (1) online measurements obtained from the installed pressure head and flow rate meters, (2) a finely tuned EPANET hydraulic model of the WDN that reliably estimates the hydraulic variables at nodes, and (3) a virtual interface that integrates the remote monitoring of the online measurements and the GA-based leak diagnosis algorithm. A remote operator interface was also designed, where remote controls allow for reconfiguration of the system remotely. The digital twin integrates both the physical and the virtualized environment. The experimental implementation of the digital twin demonstrated satisfactory results in remote monitoring and control and the diagnosis of multi-leak events.

This paper is structured as follows: Section 2 discusses the general structure of the digital twin and its main elements. Section 3 presents the specific study case, the modeling of the system, the proposed architecture, and the telecommunications design between all the involved environments. Section 3.3 presents the proposed leak diagnosis methodology and its results, and finally, Section 4 draws some conclusions and future work proposals.

2. The Digital Twin of a Hydraulic Network

According to [15], a digital twin is a part of a cyber-physical system in which a set of entities interact in a virtual space through an adequate communication network. The term cyber-physical refers to the elements of the system that are present both in the real and the virtual world, as seen in Figure 1. The data are obtained from the physical entity and sent to an information storage system using telecommunications technology. A virtualized services interface is used to access these stored data remotely (both new and historical),

which is then used to create a virtualized entity that integrates real-time operating data of the physical entity and synthetic data from real-time software-based simulations. The sensors, actuators, and controllers in the physical system are connected through the internet, which is enriched through software-based simulations and aggregated data from artificial intelligence and machine learning algorithms, as illustrated in Figure 2. Based on these concepts, in this work, a digital twin of a hydraulic network is proposed as described below.

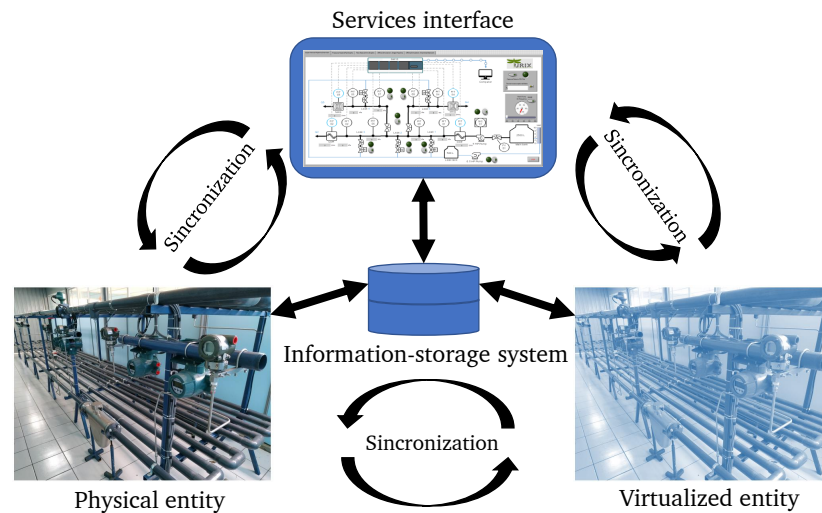


Figure 1. Interaction of the elements in the digital twin.

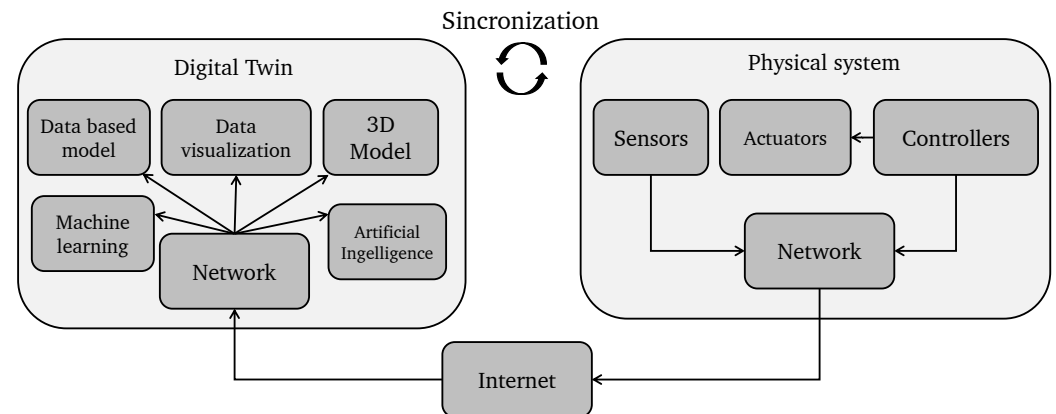


Figure 2. Main elements of the digital twin concept.

3. Description of the Hydraulic System

The digital twin was physically and virtually applied to an experimental pilot plant at the Hydroinformatics Laboratory at Instituto Tecnológico de Tuxtla Gutiérrez (see Figure 3). This experimental WDN is oriented to experimental tasks such as testing and validating control algorithms, leak diagnosis, and sensor placement techniques.

The plant is equipped with industrial instrumentation as shown on the P&ID chart given in Figure 4. The system has five electronic valves that can be remotely operated to emulate leak events, eight pressure head meters (labeled PIT-01 to PIT-08), two magnetic flow rate meters (labeled FIT-03 and FIT-04), two Coriolis-effect mass-flow meters (labeled FIT-01 and FIT-02), and one ultrasonic water-level meter installed in the storage tank (labeled LIT-01). The data acquisition is performed by a Yokogawa GM10 data-logging system connected via Ethernet with a desktop computer that uses a MATLAB-based interface to read the measurements obtained from the data-logger. A 5 hp centrifugal pump supplies the water from a main storage tank of 2500 L. The pump's rotational speed is regulated with a Micromaster 440 frequency converter that supports a maximum frequency

of 60 Hz. To guarantee the water supply, the pump frequency must be maintained over 30 Hz. Water leaked from the experiments is stored in a secondary tank with a capacity of 500 L and then recirculated to the main tank using a 0.5 hp secondary pump.



Figure 3. Test bed located at the Hydroinformatics Laboratory in Tuxtla Gutiérrez, Mexico.

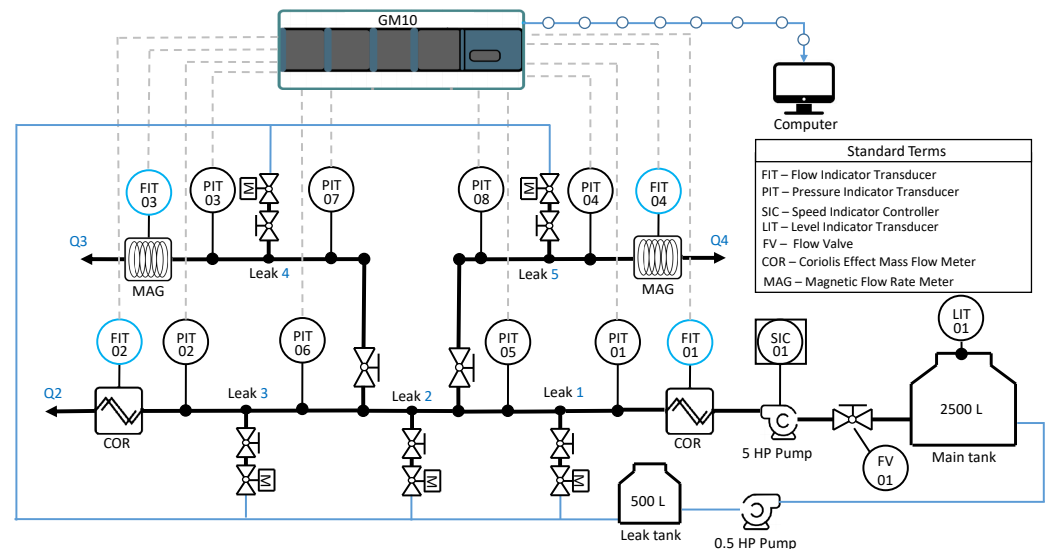


Figure 4. Pipeline and instrumentation diagram of the experimental hydraulic system.

3.1. System Modeling

An adequate hydraulic model was developed to guarantee that the estimated hydraulic variables remained reliable under different operating conditions. The hydraulic simulator EPANET was chosen for this task because of its ability to conduct simulations that closely mimic the steady-state behavior of the system while also being lightweight enough for implementation in real-time online applications. The hydraulic model is constructed as

a text file with an .inp extension, in which parameters of the topology of the system are declared, such as the location of the junction nodes of the system, the length of pipe between the junction nodes, pipe diameter, and node elevation, among others, as proposed in [16]. This text file is imported from EPANET to MATLAB 2023a[®] using the EPANET-MATLAB Toolkit provided by OpenWater Analytics [17]. This toolkit interfaces the hydraulic simulation functionalities in a coding environment, which allows the simulation of various input and consumption conditions and interfaces the model with real-world sensor readings. For simplicity, the pipeline system was discretized in pipe segments as shown in Figure 5 whose beginning and ending nodes correspond to the location of elements such as pressure meters, leak valves, or T-type fittings. The parameters corresponding to the roughness coefficient (ϵ) and the minor head-loss coefficient (K) in the pipes are estimated by the mean of a genetic algorithm as reported in our previous work in [18]. Table 1 summarizes the physical parameters for each pipe segment.

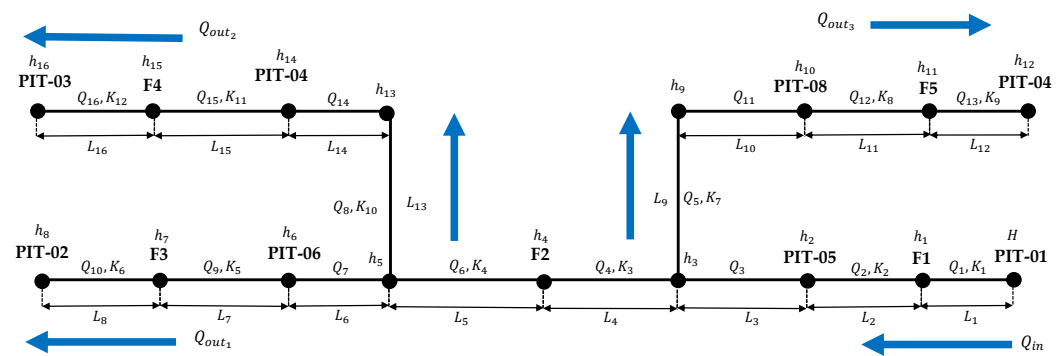


Figure 5. Modeling diagram of the pilot plant.

Table 1. Physical parameters for the modeling of the system *.

ID	Starting Node	Ending Node	L	Q	K
1	PIT-01 (H)	Leak valve 1 (h ₁)	L ₁ = 8.39 m	Q ₁	K ₁ = 2.6819
2	Leak valve 1 (h ₁)	PIT-05 (h ₂)	L ₂ = 19.75 m	Q ₂	K ₂ = 1.5034
3	PIT-05 (h ₂)	T-type fitting 1 (h ₃)	L ₃ = 0.54 m	Q ₃	0
4	T-type fitting 1 (h ₃)	Leak valve 2 (h ₄)	L ₄ = 11.31 m	Q ₄	K ₃ = 0.50473
5	Leak valve 2 (h ₄)	T-type fitting 2 (h ₅)	L ₅ = 15.91 m	Q ₆	K ₄ = 0.5030
6	T-type fitting 2 (h ₅)	PIT-06 (h ₆)	L ₆ = 0.54 m	Q ₇	0
7	PIT-06 (h ₆)	Leak valve 3 (h ₇)	L ₇ = 6.25 m	Q ₉	K ₅ = 0.5243
8	Leak valve 3 (h ₇)	PIT-02 (h ₈)	L ₈ = 21.89 m	Q ₁₀	K ₆ = 0.5201
9	T-type fitting 1 (h ₃)	T-type fitting 3 (h ₉)	L ₉ = 1.04 m	Q ₅	K ₇ = 3.9038
10	T-type fitting 3 (h ₉)	PIT-08 (h ₁₀)	L ₁₀ = 0.54 m	Q ₁₁	0
11	PIT-08 (h ₁₀)	Leak valve 6 (h ₁₁)	L ₁₁ = 19.75 m	Q ₁₂	K ₈ = 2.2308
12	Leak valve 6 (h ₁₁)	PIT-04 (h ₁₂)	L ₁₂ = 10.31 m	Q ₁₃	K ₉ = 1.7206
13	T-type fitting 2 (h ₅)	T-type fitting 4 (h ₁₃)	L ₁₃ = 1.04 m	Q ₈	K ₁₀ = 12.0158
14	T-type fitting 4 (h ₁₃)	PIT-07 (h ₁₄)	L ₁₄ = 0.54 m	Q ₁₄	0
15	PIT-07 (h ₁₄)	Leak valve 4 (h ₁₅)	L ₁₅ = 6.25 m	Q ₁₅	K ₁₁ = 1.2044
16	Leak valve 4 (h ₁₅)	PIT-03 (h ₁₆)	L ₁₆ = 23.81 m	Q ₁₆	K ₁₂ = 2.9667

* The pipeline is PVC of 2 inches schedule 80 with an inner diameter of $D = 0.0486$ m and absolute roughness $\epsilon = 2.846$ μ m.

3.2. Digital Twin Data Communication

Figure 6 shows the proposed architecture for the digital twin, which integrates three elements: the physical system, the virtualized interfaces for monitoring and diagnosis tasks, and the online cloud-based platform for data communication between the two systems.

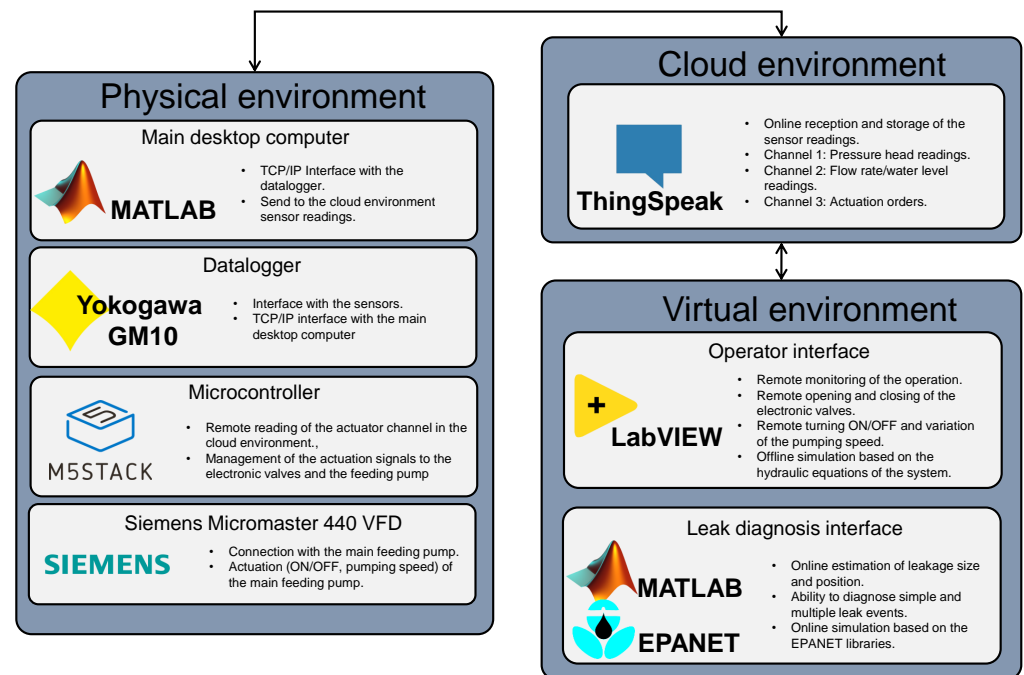


Figure 6. The proposed architecture for the digital twin.

The measured data are sent to a cloud environment via Wi-Fi using a MATLAB[®] application that connects with the GM10 and reads the measurements at the register addresses for each sensor. ThingSpeak was selected as the cloud-based storage platform. A cloud *channel* is an environment containing eight *fields* where each field can store historical measurements. The eight fields in the first channel store the measurements of the eight pressure head meters, and the first five fields in the second channel are used to store four flow rates and the water-level lectures. A third channel is used for the remote control of the actuators, with the first five fields associated with the open/closed electric valves, the sixth field associated with the on/off state of the pump, and the seventh field used to regulate the pumping speed. Figure 7 shows an example of real-time monitoring at the cloud interface of some pressure heads. Due to the latency in the telecommunications between the laboratory environment and the cloud environment, the average sampling rate is about 5 s to 15 s. This sampling rate is acceptable for this application since hydraulic systems typically have slow dynamics, and real-world implementations have lower sampling rates. All data are stored with a time mark for each variable and available for download as a .csv file.

The cloud environment comprises two interfaces: the operator and the diagnosis interfaces. Both were designed in different environments and with different objectives and applications in mind:

- The operator interface (see Figure 8) was designed in LabVIEW 2021[®], whose purpose is to control and monitor the WDN remotely. This interface includes remote controls for the electronic valves, the main feeding pump, and the operation frequency of the speed controller.
- The diagnosis interface was implemented in MATLAB[®] to perform the online leak diagnosis. As shown in Figure 9, simulated pressure heads at nodes with sensors are graphically compared with measured values at the same locations. Once a leak occurs, a mismatch between the simulated and sensor readings is perceived. The operation of the leak diagnosis algorithm will be discussed more thoroughly in Section 3.3.



Figure 7. Real-time monitoring of the pressure head in the cloud environment (Fields 1 to 4 of the pressure head cloud channel).

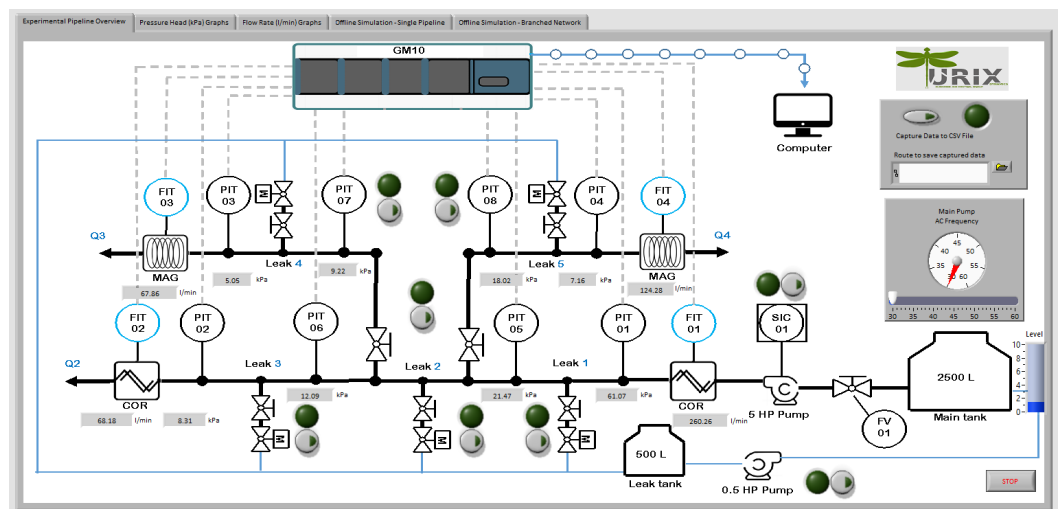
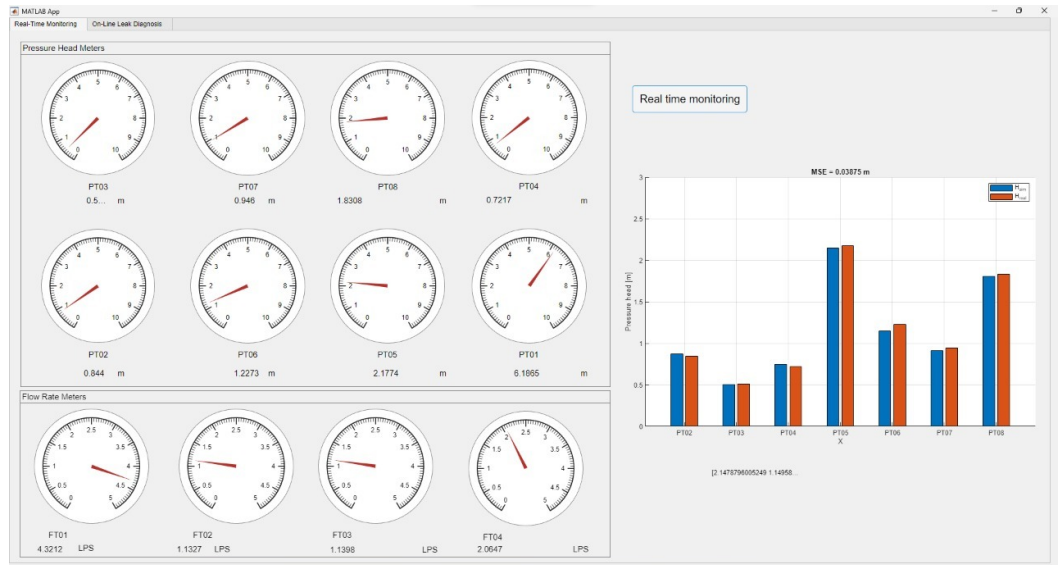


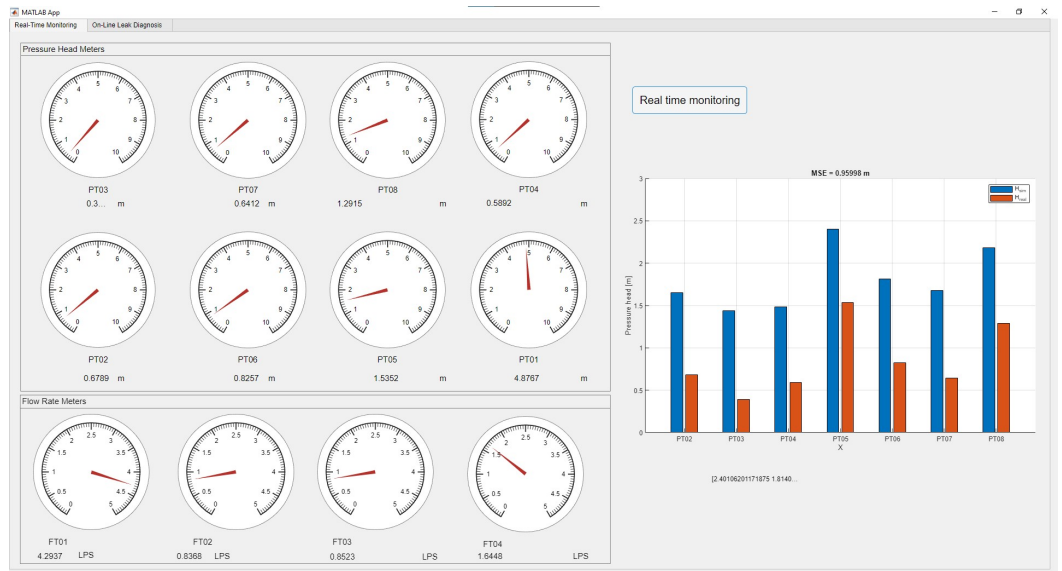
Figure 8. The operator interface of the digital twin.

Both of the interfaces rely on a low-latency telecommunications scheme. Figure 10 shows schematically the telecommunications between the digital twin environments. The installed pressure head, flow rate, and water-level data are read. A desktop computer runs a MATLAB script that interfaces with the *datalogger* using the Modbus TCP/IP protocol. Once all the readings at a given time step are available, they are sent to the cloud environment using ThingSpeak-related commands in the same MATLAB script.

The user can also interact with the remote controls implemented in the operator interface to open/close the leak valves and regulate the operating AC frequency of the main feeding pump. The on/off control orders are written in binary form (1/0) in the first six fields of the third cloud channel (five for the leak valves and one for the pump). For the case of the leak valves, a control subsystem with an embedded M5Tough microcontroller based on the ESP32 chip with Wi-Fi is used to control the open/closed state of the valves.



(a) Screenshot when no leak has been perceived.



(b) Screenshot after a leak event has been perceived.

Figure 9. Leak diagnosis interface of the digital twin.

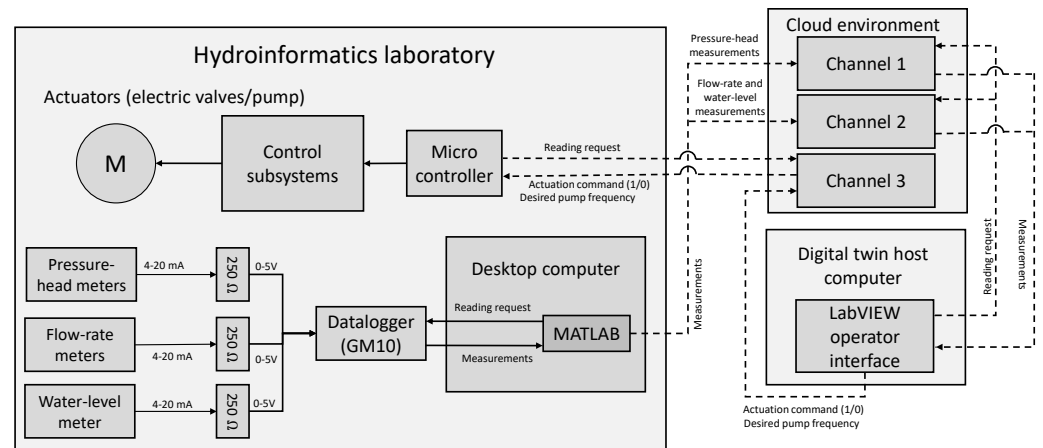


Figure 10. Telecommunications scheme between the three environments of the digital twin.

3.3. Leak Diagnosis Algorithm

The leak diagnosis methodology integrated into the proposed digital twin is based on the heuristic method of the genetic algorithm, as illustrated in Figure 11. The process begins by creating an initial population of proposed solutions called chromosomes, which can contain one or multiple genes to be calibrated. Each gene is a specific variable in the optimization problem. The fitness of every individual in the population is tested using a cost function. Those chromosomes that yield the lowest cost are selected as the best-performing individuals in the population and are used to create a new population by recombining their genes during a genetic cross-over stage. The newer generations are expected to perform better than the latter since they were created using only the genes that made up the best-performing individuals. The process continues during a defined number of generations or until the increase in the fitness of the individuals between two consecutive generations is no longer noticeable.

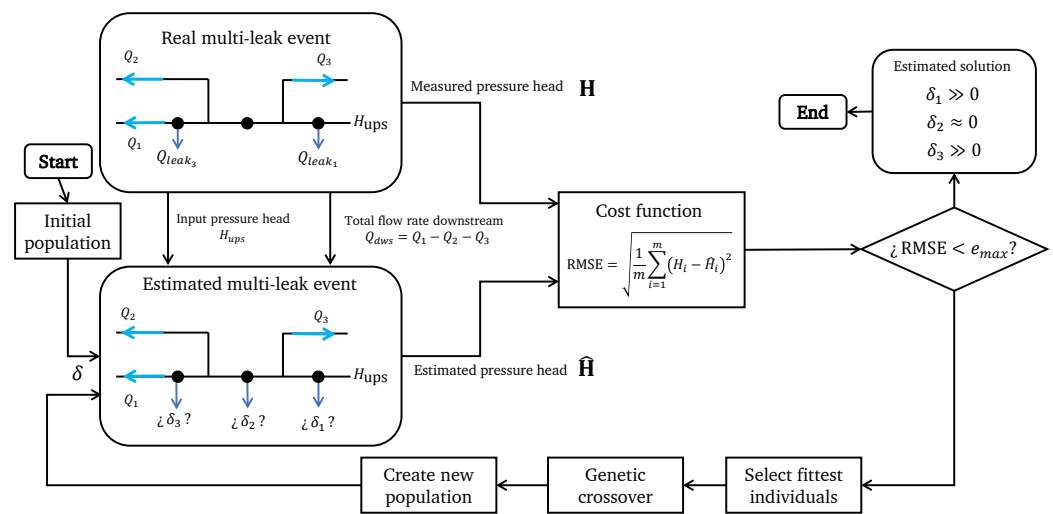


Figure 11. The process of leak diagnosis.

For our application, the pressure head and flow rate measurements are received online in the MATLAB interface that integrates the real-time measurements with the calibrated EPANET model to program the GE. A hydraulic simulation is performed considering the pressure head at upstream H_{ups} and the flow rate at downstream Q_{dws} as the initial conditions taken from the sensor readings. Figure 9a presents a real-time comparison between the sensor readings (blue columns) and the hydraulic model estimations (orange columns) at specific nodes with sensors, where it can be seen that they present a low error. Flow rate Q_{ups} is also monitored upstream, and thus the balance $Q_{ups} - Q_{dws} \approx 0$ is computed. Note that the flow balance should be as close to zero as possible without leaks, although a small deviation can be expected due to measurement noise. This deviance should be carefully characterized under leak-free conditions to avoid false alarms. Two main indicators perceive a leak event: the balance $Q_{ups} - Q_{dws} \gg 0$ and a change in the hydraulic variables such as the measured and simulated pressure head values no longer presenting a low-error fit, as can be visualized in the leak diagnosis interface as presented in Figure 9b.

Once the leak is detected, the GA process begins by calibrating the magnitude of the leak and its location. The magnitude can be easily obtained by computing the difference between upstream and downstream flow rates. However, in a multiple leak event scenario, the value Q_{leak} depends on the flow balance of all active leaks. Therefore, individual outflow in each leak node needs to be computed. The system is subdivided into pipe segments to achieve this goal. Because the leaks can occur in any number and combination of nodes, a smaller set of candidate nodes is pre-selected where the leaks are suspected to be occurring. This candidate selection needs to be thoroughly performed, considering

aspects such as the junction age and its historical leak occurrences. This is formulated as an optimization problem by considering the GA.

An important remark about the leak diagnosis methodology

In practice, leaks will typically occur at the joints (nodes) where pipe segments meet because these are the weakest points in a pipeline system. The methodology proposed in this paper assumes that leaks take place at these spatially discrete locations. However, it is not impossible that in real-world applications, a leak can be present in the *body* of the pipe rather than at its ends. In this case, the methodology proposed would still perform with an understandable error level, converging to nodes located physically close to the real leak event.

Using the GA, an optimization process occurs once a leak event has been perceived. A vector, represented as $\delta \in \mathbb{R}^n$, is created, where each element $\delta_i \in \mathbb{R}$ corresponds to the calibrated outflow value in the i -th candidate node. The proposed solutions will be structured in the following manner:

$$\delta = [\delta_1 \quad \delta_2 \quad \dots \quad \delta_n], \tag{1}$$

with n being the number of selected candidate nodes where the leaks can occur, δ_1 the calibrated outflow for the first candidate node, δ_2 the calibrated outflow for the second candidate node, and so on. Adequate lower (lb) and upper (ub) bounds are selected for the GA-driven search to create these δ_i values, following the restrictions

$$\begin{aligned} lb &= 0 \\ ub &= Q_{leak} \\ \sum_{i=1}^n \delta_i &= Q_{ups} - Q_{dws} = Q_{leak} \end{aligned} \tag{2}$$

After the initial population is created, the fitness of each candidate is tested by evaluating the error between the measured and estimated pressure heads after the multi-leak event as follows:

1. The δ_i values in a given solution vector are set in the EPANET model as the actual outflow in their corresponding nodes. The latest readings for H_{ups} , and Q_{dws} are also set as the initial conditions in the EPANET model, and a steady-state hydraulic simulation is performed.
2. From the simulation, the following is obtained:

$$\hat{\mathbf{H}} = [\hat{H}_1 \quad \hat{H}_2 \quad \dots \quad \hat{H}_m], \tag{3}$$

where m is the number of nodes with sensors and \hat{H}_i is the estimation of the pressure head at the i -th node with sensor. Similarly, a vector containing the measured pressure head at the same nodes is constructed as follows:

$$\mathbf{H} = [H_1 \quad H_2 \quad \dots \quad H_m], \tag{4}$$

3. The fitness is evaluated in terms of the root of the mean squared error (RMSE):

$$RMSE = \sqrt{\frac{1}{m} \sum_{i=1}^m (H_i - \hat{H}_i)^2}, \tag{5}$$

4. The fitness of all individuals in the generation is tested, and those that provide the lowest RMSE are selected for the genetic crossover stage. A new generation of proposed solutions is created, and the algorithm returns to step 1.

After the optimization process has finished, it is expected that the calibrated δ_i values corresponding to the nodes with actual leaks will be calibrated significantly greater than zero. In contrast, those corresponding to nodes where the leak event is not happening will be estimated with a value close to zero.

For any multi-leak scenario, the input pressure head and the total combined flow rate downstream are fed to the hydraulic simulator and the initial δ values population. After the hydraulic simulation is computed, the fitness of each element is calculated. If any computed RMSE is less than a pre-set tolerance value e_{min} , the search finishes, and the solution vector is selected as the estimated multi-leak scenario. Otherwise, the GA continues, and the fittest individuals in the population are selected, such that the genetic crossover takes place and a new generation is created to continue with the search. After the GA-based search is performed, the δ values corresponding to the nodes without leaks are expected to be calibrated closely to zero. In contrast, the nodes with actual leaks will be calibrated with outflows significantly greater than zero. After the outflows are calibrated, the nodes with the greater leaked flow rates are selected as the leaky nodes and presented graphically to the user.

3.4. Experimental Validation

The experimental demonstration of the proposed leak diagnosis method was performed by considering that leaks take place only in the main pipeline section of the system since it was observed that inducing an outflow at this location causes a much more noticeable pressure head drop than leaks occurring in the branches. Since three leak valves are installed in the main pipeline section of the system, different multi-leak scenarios were proposed and tested: the scenario \mathcal{A} for a combined leak event considering two simultaneous leaks occurring in valves 1 and 2, the scenario \mathcal{B} considering that leaks take place in valves 1 and 3, and finally, the scenario \mathcal{C} with two simultaneous leaks in valves 2 and 3.

Figure 12 shows the diagnosis results for scenario \mathcal{A} . Both leak valves are opened at $t \approx 60$ [s]. Once the leak is perceived, the δ values are calibrated. It can be seen in Figure 12 how the values corresponding to δ_1 and δ_2 are significantly greater than δ_3 , which in turn remains close to zero for the duration of the experiment. This demonstrates that, as expected, the leaks are located at positions 1 and 2.

Multiple tests were performed to demonstrate that the proposed methodology remains valid under repeated experiments. Table 2 summarizes the obtained results for the three tests conducted for scenario \mathcal{A} . It can be seen how the calibrated δ_1 and δ_2 values are greater (of various orders of magnitude) than δ_3 for all cases.

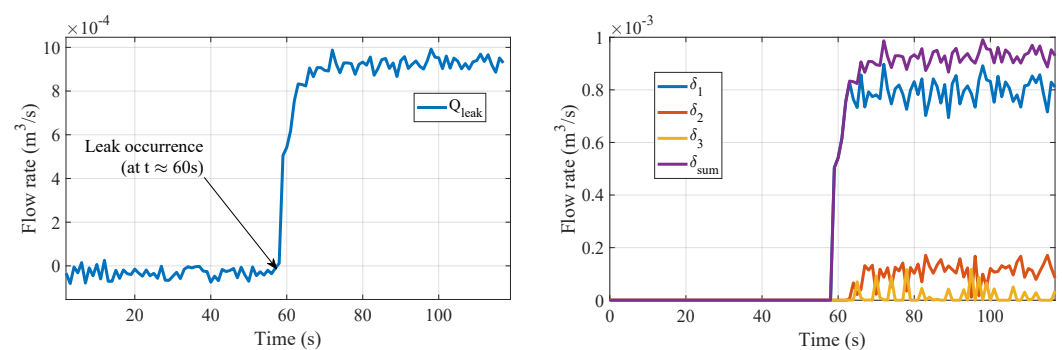


Figure 12. Leak diagnosis results for scenario \mathcal{A} .

Table 2. Multi-leak scenario \mathcal{A} : Experimental results for repeated experiments.

Experiment	δ_1	δ_2	δ_3
$\mathcal{A}.1$	$8.3208 \times 10^{-4} \text{ m}^3/\text{s}$	$1.2012 \times 10^{-4} \text{ m}^3/\text{s}$	$8.2972 \times 10^{-11} \text{ m}^3/\text{s}$
$\mathcal{A}.2$	$8.4016 \times 10^{-4} \text{ m}^3/\text{s}$	$9.7469 \times 10^{-5} \text{ m}^3/\text{s}$	$4.241 \times 10^{-11} \text{ m}^3/\text{s}$
$\mathcal{A}.3$	$8.5167 \times 10^{-4} \text{ m}^3/\text{s}$	$1.0053 \times 10^{-4} \text{ m}^3/\text{s}$	$2.4946 \times 10^{-9} \text{ m}^3/\text{s}$

Similar validation tests were conducted for multi-leak scenarios \mathcal{B} and \mathcal{C} , obtaining satisfactory results in all tests in the isolation of the correct leak events and in quantifying the leaked outflow. Results can be consulted in Figures 13 and 14 as well as in Tables 3 and 4. Notice how for scenario \mathcal{B} the calibrated δ_2 value will be significantly smaller than δ_1 and δ_3 , whereas for scenario \mathcal{C} , δ_1 is, as would be expected, the lowest-calibrated value.

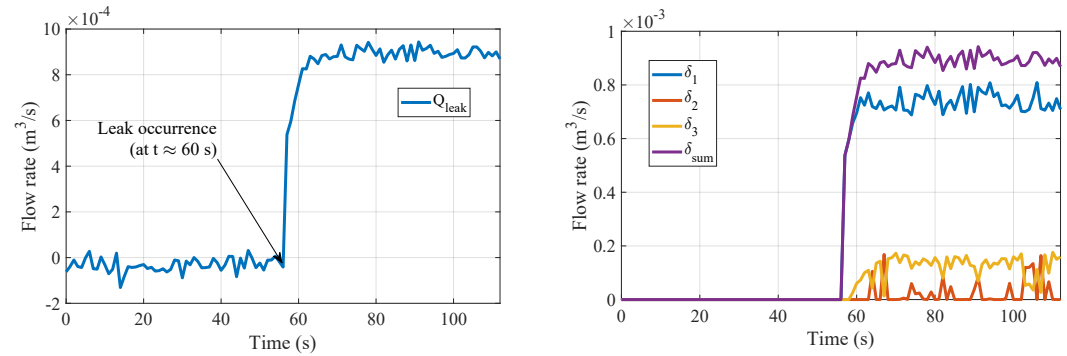


Figure 13. Leak diagnosis results for scenario \mathcal{B} .

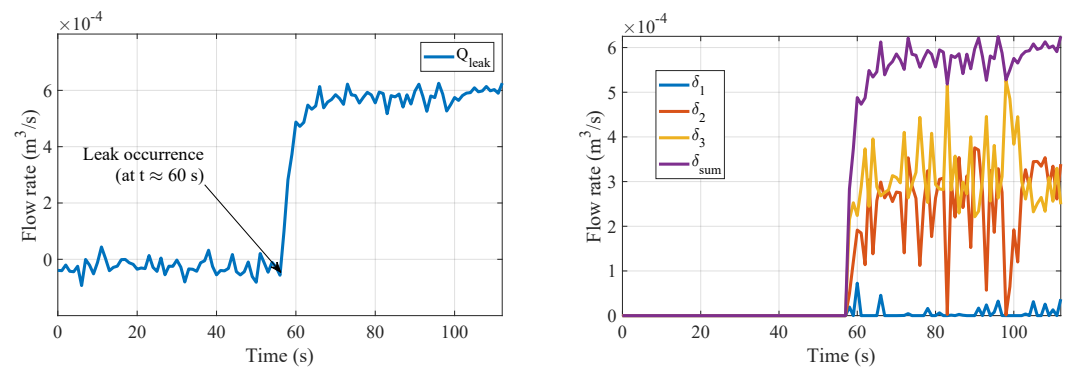


Figure 14. Leak diagnosis results for scenario \mathcal{C} .

Table 3. Multi-leak scenario \mathcal{B} : Experimental results for repeated experiments.

Dataset	δ_1	δ_2	δ_3
$\mathcal{B}.1$	$7.4552 \times 10^{-4} \text{ m}^3/\text{s}$	$1.2901 \times 10^{-10} \text{ m}^3/\text{s}$	$1.522 \times 10^{-4} \text{ m}^3/\text{s}$
$\mathcal{B}.2$	$7.8831 \times 10^{-4} \text{ m}^3/\text{s}$	$7.2587 \times 10^{-13} \text{ m}^3/\text{s}$	$1.3544 \times 10^{-4} \text{ m}^3/\text{s}$
$\mathcal{B}.3$	$8.0057 \times 10^{-4} \text{ m}^3/\text{s}$	$4.8458 \times 10^{-10} \text{ m}^3/\text{s}$	$1.2764 \times 10^{-4} \text{ m}^3/\text{s}$

Table 4. Multi-leak scenario \mathcal{C} : Experimental results for repeated experiments.

Dataset	δ_1	δ_2	δ_3
$\mathcal{C}.1$	$3.061 \times 10^{-11} \text{ m}^3/\text{s}$	$3.5082 \times 10^{-4} \text{ m}^3/\text{s}$	$2.4798 \times 10^{-4} \text{ m}^3/\text{s}$
$\mathcal{C}.2$	$2.9279 \times 10^{-5} \text{ m}^3/\text{s}$	$3.5794 \times 10^{-4} \text{ m}^3/\text{s}$	$2.2387 \times 10^{-4} \text{ m}^3/\text{s}$
$\mathcal{C}.3$	$2.8718 \times 10^{-5} \text{ m}^3/\text{s}$	$3.7529 \times 10^{-4} \text{ m}^3/\text{s}$	$2.1646 \times 10^{-4} \text{ m}^3/\text{s}$

The operation of the digital twin can be seen in the Youtube video at the link <https://youtu.be/fN-sNN2qV0c>, accessed on 16 October 2023.

4. Conclusions

This paper presents the implementation of the digital twin of a hydraulic system for leak diagnosis applications. The system integrates IoT technology to remotely control and monitor the system variables, sensors, and actuators. The communications between the DT and the hydraulic system present an acceptable latency, allowing the integration of

an online leak diagnosis method based on a genetic algorithm approach. This method considers online measurements to calibrate the magnitude and the leak location. Future work will be performed to replicate this method on a sector of a hydraulic network by considering other telemetry methods that use cellular networks, such as GSM or 4G, instead of a local Wi-Fi communication network.

Author Contributions: Conceptualization, L.G.-C., I.S.-R. and F.-R.L.-E.; methodology, L.G.-C. and I.S.-R.; software, L.G.-C., I.S.-R. and F.-R.L.-E.; validation, L.G.-C. and S.G.-P.; formal analysis, L.G.-C., I.S.-R., E.E.-G. and F.-R.L.-E.; data curation, L.G.-C. and S.G.-P.; writing—original draft preparation, L.G.-C., I.S.-R., L.T. and F.-R.L.-E.; writing—review and editing, L.G.-C. and I.S.-R.; visualization, L.G.-C.; supervision, I.S.-R. and F.-R.L.-E.; project administration, F.-R.L.-E. and I.S.-R. All authors have read and agreed to the published version of the manuscript.

Funding: This research has been supported by the Consejo Nacional de Humanidades, Ciencias y Tecnologías (CONAHCyT) and by Tecnológico Nacional de México under the program *Fortalecimiento de Cuerpos Académicos PRODEP 2023* and the project 17937.23-P.

Data Availability Statement: Data available on request.

Conflicts of Interest: The authors declare no conflict of interest.

References

- Romano, O.; Akhmouch, A. Water Governance in Cities: Current Trends and Future Challenges. *Water* **2019**, *11*, 500. [[CrossRef](#)]
- OECD. *Water Governance in Cities*; OECD: Paris, France, 2016; p. 140. [[CrossRef](#)]
- Navarro, A.; Delgado-Aguiñaga, J.A.; Sánchez-Torres, J.D.; Begovich, O.; Besançon, G. Evolutionary Observer Ensemble for Leak Diagnosis in Water Pipelines. *Processes* **2019**, *7*, 913. [[CrossRef](#)]
- Lin, J.; Sedigh, S.; Miller, A. Towards Integrated Simulation of Cyber-Physical Systems: A Case Study on Intelligent Water Distribution. In Proceedings of the 2009 Eighth IEEE International Conference on Dependable, Autonomic and Secure Computing, Chengdu, China, 12–14 December 2009; pp. 690–695. [[CrossRef](#)]
- Wang, Z.; Song, H.; Watkins, D.W.; Ong, K.G.; Xue, P.; Yang, Q.; Shi, X. Cyber-physical systems for water sustainability: Challenges and opportunities. *IEEE Commun. Mag.* **2015**, *53*, 216–222. [[CrossRef](#)]
- Radhakrishnan, V.; Wu, W. IoT Technology for Smart Water System. In Proceedings of the 2018 IEEE 20th International Conference on High Performance Computing and Communications; IEEE 16th International Conference on Smart City; IEEE 4th International Conference on Data Science and Systems (HPCC/SmartCity/DSS), Exeter, UK, 28–30 June 2018; pp. 1491–1496. [[CrossRef](#)]
- Torres, L. IoT stations for monitoring a district metered area of Guanajuato city. In Proceedings of the 2021 IEEE International Conference on Engineering Veracruz (ICEV), Boca del Rio, Mexico, 26–29 October 2021; pp. 1–6. [[CrossRef](#)]
- Pacheco, J.; Ibarra, D.; Vijay, A.; Hariri, S. IoT Security Framework for Smart Water System. In Proceedings of the 2017 IEEE/ACS 14th International Conference on Computer Systems and Applications (AICCSA), Hammamet, Tunisia, 30 October–3 November 2017; pp. 1285–1292. [[CrossRef](#)]
- Kartakis, S.; Abraham, E.; McCann, J.A. WaterBox: A Testbed for Monitoring and Controlling Smart Water Networks. In Proceedings of the 1st ACM International Workshop on Cyber-Physical Systems for Smart Water Networks, New York, NY, USA, 27 February 2015. [[CrossRef](#)]
- El Sayed, H.Y.; Al-Kady, M.; Siddik, Y. Management of Smart Water Treatment Plant using IoT Cloud Services. In Proceedings of the 2019 International Conference on Smart Applications, Communications and Networking (SmartNets), Sharm El Sheikh, Egypt, 17–19 December 2019; pp. 1–5. [[CrossRef](#)]
- Alghamdi, R.; Sharma, S.K. IoT-Based Smart Water Management Systems for Residential Buildings in Saudi Arabia. *Processes* **2022**, *10*, 2462. [[CrossRef](#)]
- Conejos Fuertes, P.; Martínez Alzamora, F.; Hervás Carot, M.; Alonso Campos, J. Building and exploiting a Digital Twin for the management of drinking water distribution networks. *Urban Water J.* **2020**, *17*, 704–713. [[CrossRef](#)]
- Ferra Mesquida, M. Digital Twin in Water Distribution Networks. Ph.D. Thesis, UPC, Escola Tècnica Superior d'Enginyeria Industrial de Barcelona, Departament d'Organització d'Empreses, Barcelona, Spain, 2021.
- Pesantez, J.E.; Alghamdi, F.; Sabu, S.; Mahinthakumar, G.; Berglund, E.Z. Using a digital twin to explore water infrastructure impacts during the COVID-19 pandemic. *Sustain. Cities Soc.* **2022**, *77*, 103520. [[CrossRef](#)] [[PubMed](#)]
- Schroeder, G.N.; Steinmetz, C.; Pereira, C.E.; Espindola, D.B. Digital Twin Data Modeling with AutomationML and a Communication Methodology for Data Exchange. *IFAC-PapersOnLine* **2016**, *49*, 12–17. [[CrossRef](#)]
- Rossman, L.A.; Woo, H.; Tryby, M.; Shang, F.; Janke, R.; Haxton, T. *EPANET 2.2 User Manual*; Technical Report EPA/600/R-20/133; U.S. Environmental Protection Agency: Washington, DC, USA, 2020.

17. Eliades, D.G.; Kyriakou, M.; Vrachimis, S.; Polycarpou, M.M. EPANET-MATLAB Toolkit: An Open-Source Software for Interfacing EPANET with MATLAB. *Zenodo* **2017**, *1*, 1493. [[CrossRef](#)]
18. Gómez-Coronel, L.; Santos-Ruiz, I.; Torres, L.; López-Estrada, F.; Delgado-Aguinaga, J. Model Calibration for a Hydraulic Network Using Genetic Algorithms. In *Memorias del Congreso Nacional de Control Automático*; Congreso Nacional de Control Automático: Tuxtla Gutiérrez, Mexico, 2022; pp. 146–251. [[CrossRef](#)]

Disclaimer/Publisher's Note: The statements, opinions and data contained in all publications are solely those of the individual author(s) and contributor(s) and not of MDPI and/or the editor(s). MDPI and/or the editor(s) disclaim responsibility for any injury to people or property resulting from any ideas, methods, instructions or products referred to in the content.